



PD-L1+ tumor-associated macrophages and PD-1+ tumor infiltrating lymphocytes predict survival in primary testicular lymphoma

by Marjukka Pollari, Oscar Brück, Teijo Pellinen, Pauli Vähämurto, Marja-Liisa Karjalainen-Lindsberg, Susanna Mannisto, Olli Kallioniemi, Pirkko-Liisa Kellokumpu-Lehtinen, Satu Mustjoki, Suvi-Katri Leivonen, and Sirpa Leppä

Haematologica 2018 [Epub ahead of print]

Citation: Marjukka Pollari, Oscar Brück, Teijo Pellinen, Pauli Vähämurto, Marja-Liisa Karjalainen-Lindsberg, Susanna Mannisto, Olli Kallioniemi, Pirkko-Liisa Kellokumpu-Lehtinen, Satu Mustjoki, Suvi-Katri Leivonen, and Sirpa Leppä. PD-L1+ tumor-associated macrophages and PD-1+ tumor infiltrating lymphocytes predict survival in primary testicular lymphoma. Haematologica. 2018; 103:xxx doi:10.3324/haematol.2018.197194

Publisher's Disclaimer.

E-publishing ahead of print is increasingly important for the rapid dissemination of science. Haematologica is, therefore, E-publishing PDF files of an early version of manuscripts that have completed a regular peer review and have been accepted for publication. E-publishing of this PDF file has been approved by the authors. After having E-published Ahead of Print, manuscripts will then undergo technical and English editing, typesetting, proof correction and be presented for the authors' final approval; the final version of the manuscript will then appear in print on a regular issue of the journal. All legal disclaimers that apply to the journal also pertain to this production process.

PD-L1⁺ tumor-associated macrophages and PD-1⁺ tumor infiltrating lymphocytes predict survival in primary testicular lymphoma

Marjukka Pollari^{1,2}, Oscar Brück³, Teijo Pellinen⁴, Pauli Vähämurto^{1,5}, Marja-Liisa Karjalainen-Lindsberg⁶, Susanna Mannisto^{1,5}, Olli Kallioniemi^{4,7}, Pirkko-Liisa Kellokumpu-Lehtinen^{2,8}, Satu Mustjoki^{3,9}, Suvi-Katri Leivonen^{1,5} and Sirpa Leppä^{1,5}

¹*Research Program Unit, Faculty of Medicine, University of Helsinki, Helsinki, Finland;*

²*Department of Oncology, Tampere University Hospital, Tampere, Finland;*

³*Hematology Research Unit Helsinki, Department of Clinical Chemistry and Hematology, University of Helsinki, Helsinki, Finland;*

⁴*Institute for Molecular Medicine Finland (FIMM), Helsinki, Finland;*

⁵*Department of Oncology, Comprehensive Cancer Center, Helsinki University Hospital, Helsinki, Finland;*

⁶*Department of Pathology, Helsinki University Hospital, Helsinki, Finland;*

⁷*Science for Life Laboratory, Karolinska Institutet, Department of Oncology and Pathology, Solna, Sweden;*

⁸*Faculty of Medicine and Life Sciences, University of Tampere, Tampere, Finland;*

⁹*Department of Hematology, Comprehensive Cancer Center, Helsinki University Hospital, Helsinki, Finland*

Running head: Tumor-associated macrophages in PTL

Corresponding author:

Sirpa Leppä, MD, Professor

Department of Oncology

Helsinki University Hospital Comprehensive Cancer Center

P.O. Box 180

FI-00029 Helsinki, Finland

Email: sirpa.leppa@helsinki.fi

Phone: +358 40 7558293

Word count abstract: 248

Word count main text: 2457

Figures: 2

Tables: 4

Supplementary files: 1

Acknowledgements:

We thank Drs. Petri Auvinen and Lars Paulin (Institute of Biotechnology, University of Helsinki), Finland for the Nanostring analyses. Anne Aarnio and Marika Tuukkanen are acknowledged for technical assistance.

Abstract

Primary testicular lymphoma is a rare and aggressive lymphoid malignancy, most often representing diffuse large B-cell lymphoma histologically. Tumor-associated macrophages and tumor-infiltrating lymphocytes have been associated with survival in diffuse large B-cell lymphoma, but their prognostic impact in primary testicular lymphoma is unknown. Here, we aimed to identify macrophages, their immunophenotypes and association with lymphocytes, and translate the findings into survival of patients with primary testicular lymphoma. We collected clinical data and tumor tissue from 74 primary testicular lymphoma patients, and used multiplex immunohistochemistry and digital image analysis to examine macrophage markers (CD68, CD163, and c-Maf), T-cell markers (CD3, CD4, and CD8), B-cell marker (CD20), and three checkpoint molecules (PD-L1, PD-L2, and PD-1). We demonstrate that a large proportion of macrophages (median 41%, range 0.08-99%) and lymphoma cells (median 34%, range 0.1-100%) express PD-L1. The quantity of PD-L1⁺CD68⁺ macrophages correlates positively with the amount of PD-1⁺ lymphocytes, and a high proportion of either PD-L1⁺CD68⁺ macrophages or PD-1⁺CD4⁺ and PD-1⁺CD8⁺ T-cells translates into favorable survival. In contrast, the number of PD-L1⁺ lymphoma cells or PD-L1⁻ macrophages do not associate with outcome. In multivariate analyses with IPI, PD-L1⁺CD68⁺ macrophage and PD-1⁺ lymphocyte contents remain as independent prognostic factors for survival. In conclusion, high PD-L1⁺CD68⁺ macrophage and PD-1⁺ lymphocyte contents predict favorable survival in patients with primary testicular lymphoma. The findings implicate that the tumor microenvironment and PD-1 – PD-L1 pathway have a significant role in regulating treatment outcome. They also bring new insights to the targeted therapy of primary testicular lymphoma.

Introduction

Primary testicular lymphoma (PTL) is a rare and aggressive lymphoid malignancy affecting mainly elderly men. The biology of PTL is beginning to emerge,¹⁻⁷ and the outcome has improved with the addition of anthracycline-based chemotherapy, central nervous system (CNS) targeted therapy and irradiation of the contralateral testis.⁸⁻¹⁰ Majority of PTLs represent diffuse large B-cell lymphoma (DLBCL) displaying more often non-germinal center B-cell (GCB) than GCB-like signatures.¹¹ Somatic mutations in NF-kappa-B pathway genes, such as *MYD88* and *CD79B*, as well as rearrangements of programmed cell death ligand (PD-L) -1 and -2 genes, have been shown to be enriched in PTL.^{2, 4} In addition, two stromal signatures associated with outcome have been described in primary, mainly nodal DLBCL patients treated with immunochemotherapy, forming a backbone for our study.¹²

We have recently demonstrated that tumor-associated macrophages (TAMs) have a favorable prognostic impact on survival in DLBCL patients after immunochemotherapy,¹³ whereas other groups have investigated the role of programmed cell death-1 (PD-1) pathway in DLBCL.¹⁴⁻¹⁸ While PD-1 protein is expressed predominantly by activated tumor-infiltrating lymphocytes (TILs), its ligands (PD-L1 and PD-L2) have been shown to be expressed both by the tumor cells and the tumor microenvironment.^{15, 19-21} An unexpected feature has been that PD-L1 expression by the tumor-infiltrating myeloid and other immune cells can be more prevalent than PD-L1 expression by the tumor cells.^{15, 19, 20} Recently, it was also shown that the expression of PD-L1 not only by the tumor cells but also by the host cells plays a critical role in mediating the immunosuppressive function of the PD-1 pathway.²¹

In DLBCL, expression of PD-L1 by lymphoma cells has been associated with poor outcome.¹⁴

Interestingly, 9p24.1/*PD-L1*/*PD-L2* copy number alterations and additional translocations of these loci are frequent in PTLs (>50%), leading to increased expression of the PD-Ls,⁴ and possibly also to immune escape. Whether the expression of PD-1 and PD-Ls predict survival in PTL, and in which compartments, is unknown.

With the aim of resolving the relative expression of checkpoint molecules by the tumor and host immune cells in patients with PTL, we examined B-cells, TAMs, TILs, and checkpoint molecules by using multiplex immunohistochemistry (mIHC),²² allowing simultaneous detection of CD68⁺ TAMs, CD163⁺ or c-Maf⁺ M2-polarized TAMs, CD4⁺ and CD8⁺ T-cells, CD20⁺ B-cells, and the checkpoint molecules PD-L1, PD-L2 and PD-1. The findings were correlated with clinical parameters and survival.

Methods

Patients

We identified 74 PTL patients with DLBCL histology diagnosed between the years 1987 and 2013 from the pathology databases of the University Hospitals in Southern Finland. Histological diagnosis was established from surgical pretreatment tumor tissue according to current criteria of the World Health Organization (WHO) classification.²³ Majority of the patients were treated with anthracycline based chemotherapy. About half of the patients received rituximab as a part of their treatment. Contralateral testis was treated with surgical excision or irradiation for a minority of the patients. Patients were divided into three equal tertiles, based on the content of different immune cell subtypes (high, intermediate, low). The patient characteristics are described in more

detail in Table 1. The protocol and sampling were approved by the Institutional Review Boards, Ethics Committees and Finnish National Supervisory Authority for Welfare and Health.

Multiplex immunohistochemistry (mIHC)

Formalin-fixed, paraffin-embedded (FFPE) primary tumor tissues were collected from the local biobanks and reviewed to match the latest WHO classification.²³ Selection of the cores on the tissue microarray (TMA) was based on the evaluation of a hematopathologist. TMA was constructed and the sections (3.5 µm) stained with 4-plex primary antibody panels (PD-L1, PD-L2, CD68, c-MAF; CD3, CD4, CD8, PD-1; CD20, CD163, PD1, PD-L1; Supplementary Table 1), followed by fluorescently labelled secondary antibodies and DAPI counterstain (nuclear stain). A more detailed description of the stainings is provided in the Supplementary Methods. Fluorescent images were acquired with AxioImager.Z2 (Zeiss, Germany). Machine-learning platform CellProfiler²⁴ 2.1.2 was used for cell segmentation, intensity measurements (upper quartile intensity) and immune cell classification. Different cell types were quantified as proportion to all cells (e.g. PD-L1⁺CD68⁺ implying the number of PD-L1⁺CD68⁺ TAMs from all cells in a TMA spot) or as a proportion to a specific cell subtype (e.g. PD-L1⁺CD68⁺/CD68⁺ implying the number of PD-L1⁺CD68⁺ cells from all CD68⁺ TAMs). Spots with less than 5000 cells were excluded from the analysis, and data from duplicate spots from the same patient were merged.

Gene expression analysis

CD68, *CD163*, *MAF*, *MS4A1* (CD20), *CD274* (PD-L1), *PDCD1LG2* (PD-L2), and *PDCD1* (PD-1) mRNA levels were measured from 60 PTL samples using digital gene expression analysis with NanoString nCounter (Nanostring Technologies, Seattle, WA).²⁵

Survival definitions and statistical analyses

Overall survival (OS) was defined as time between diagnosis and death from any cause, disease specific survival (DSS) as time between diagnosis and lymphoma related death, and progression free survival (PFS) as time between diagnosis and lymphoma progression or death from any cause. Statistical analyses were performed with IBM SPSS v.24.0 (IBM, Armonk, NY, USA). Differences in the frequency of prognostic factors between three patient groups were analyzed by Kruskal-Wallis test. Correlations between gene expression values and cell counts as well as between different immune cell subpopulations were tested with Spearman's rank correlation.

Survival rates were estimated using the Kaplan–Meier method. Univariate and multivariate analyses were performed according to the Cox proportional hazards regression model. The potential bias due to duration of follow-up was assessed by Schoenfeld residual. Probability values below 0.05 were considered statistically significant. All comparisons and all comparative tests were two-tailed.

Results

Patient characteristics

Patient and treatment characteristics of the study cohort are shown in Table 1. Majority of the patients represented non-GCB phenotype, low stage, and had low/intermediate International Prognostic Index (IPI). Altogether 34 deaths, 24 relapses and 24 lymphoma-associated deaths occurred during the median follow-up of 67 months (range from 6.7 to 120 months). Five-year OS, DSS and PFS rates were 56%, 68%, and 53%, respectively.

Association of CD68, PD-L1 and PD-L2 encoding gene expression with survival

First, we determined the gene expression of the macrophage markers (*CD68*, *CD163* and *MAF*), checkpoint molecules *CD274* (PD-L1), *PDCD1LG2* (PD-L2) and *PDCD1* (PD-1), and the B-cell marker *MS4A1* (CD20). *CD68* expression correlated positively with *CD274* ($r_s=0.654$, $p<0.001$), *PDCD1LG2* ($r_s=0.636$, $p<0.001$), *CD163* ($r_s=0.602$, $p<0.001$), and *MAF* ($r_s=0.425$, $p=0.001$) levels, and to a lesser extent with *PDCD1* ($r_s=0.300$, $p=0.020$), whereas no correlation between *CD68* and *MS4A1* expression was found. Furthermore, the expression of *CD68*, *CD274* and *PDCD1LG2* genes analyzed as continuous variables, but not *PDCD1*, *CD163* or *MAF*, translated into favorable survival (Table 2).

High PD-L1⁺ TAM content predicts favorable survival

To explore the expression of the checkpoint molecules in the tumor cells and in the microenvironment in more detail, we analyzed the cell immunophenotypes with mIHC from a PTL TMA using four primary antibodies and DAPI (nuclear stain) simultaneously (Figure 1A-C; see also Table 1 for the TMA cohort used and Supplementary Table 1 for the antibody panels). The marker CD68 was used to identify all TAMs. Subpopulations of TAMs were defined by the presence and absence of CD163, c-MAF, PD-L1 and PD-L2 (Figure 1A-B, D). In addition, CD20 marker was used to identify lymphoma cells (Figure 1B). For detecting TILs, a panel with CD3, CD4, CD8, and PD1 antibodies was used (Figure 1C).

As a proof of concept, we found high agreement with the gene expression and the mIHC data when analyzing the quantities of CD68⁺ macrophages ($r_s=0.637$, $p<0.001$), lymphoma cells ($r_s=0.704$, $p<0.001$) and PD-L1⁺ cells ($r_s=0.710$, $p<0.001$) (Supplementary Figure 1). The proportions of the different cell types in the tumor tissue are shown in Figure 1D. The most prominent non-

malignant cell type was CD3⁺ T-lymphocyte (median 45%, range 5-97%). TAM and PD-L1⁺ cell contents showed a great variation between the samples (CD68⁺ TAMs, median 23%, range 3-81%; PD-L1⁺ cells, median 15%, range 0.01-100%), and a large proportion of lymphoma cells (median 34%, range 0.1-100%) and TAMs (median 41%, range 0.1-99%) expressed PD-L1. Due to a low proportion of PD-L2⁺ cells (0.06%) (data not shown), PD-L2 was excluded from further analyses.

We further observed that high number of PD-L1⁺ cells, high proportion of PD-L1⁺CD68⁺ macrophages from all cells, as well as high proportion of PD-L1⁺CD68⁺ macrophages from all CD68⁺ macrophages (PD-L1⁺CD68⁺/CD68⁺), associated with favorable OS when analyzed as continuous variables (Table 3). In order to use an objective cutoff we stratified the patients into three equal subgroups based on tertiles of the PD-L1⁺CD68⁺ macrophage counts (high, intermediate, low). The 5-year OS and DSS rates were clearly worse for the patients with low number of PD-L1⁺CD68⁺ macrophages ($\leq 4.75\%$ corresponding to the lowest tertile of the patients) in comparison to the patients with intermediate or high numbers ($> 4.75\%$, 5-y OS, 39% vs 66%, $p=0.014$; 5-y DSS, 53% vs 76%, $p=0.056$; Figure 2A). When PD-L1⁺CD68⁺ macrophage count was included in a multivariate analysis with IPI, both factors had independent prognostic value for OS (Table 4). In contrast, neither PD-L1⁺ lymphoma cells, PD-L1⁺CD68⁻ cells nor any other TAM phenotypes were significantly associated with survival (Table 3). When comparing the three PD-L1⁺CD68⁺ TAM subgroups (high, intermediate and low), no significant differences in age, molecular subtype, IPI score or treatments were observed (Table 1). However, high PD-L1⁺CD68⁺ macrophage count was associated with limited disease stage. When the patients treated in the pre-rituximab era were removed from the analyses, a trend towards worse survival was maintained for the patients with low number of PD-L1⁺CD68⁺ macrophages ($\leq 5.97\%$, the lowest tertile; OS, $p=0.093$,

Supplementary Figure 2A). These results highlight the clinical relevance and possible functional connection of PD-L1+ TAMs for PTL progression.

Association of PD1⁺ TILs with survival

Given the prognostic value of PD-L1⁺ TAMs, we then determined their association with T-cells by mIHC. The marker CD3 was used to identify all T cells. Subpopulations of T cells were then defined by the presence and absence of CD4, CD8 and PD1 (Figure 1C-D). As with CD4⁺ T-helper and CD8⁺ cytotoxic cells in general, PD-1⁺CD3⁺CD4⁺ and PD-1⁺CD3⁺CD8⁺ T-cell counts correlated with the PD-L1⁺ TAM counts (Supplementary Table 2). Furthermore, as overall with T-cells²⁵ high and intermediate number of PD-1⁺ CD4⁺ and CD8⁺ T-cells associated with superior survival (PD-1⁺CD3⁺CD4⁺ cells ≤5.7% corresponding to the lowest tertile vs other patients; 5-y OS, 34% vs 68%, p=0.002; 5-y DSS, 43% vs 81%, p<0.001; PD-1⁺CD3⁺CD8⁺ cells, ≤7.2% corresponding to the lowest tertile vs other patients; 5-y OS, 39% vs 65%, p=0.008; 5-y DSS, 43% vs 81%, p<0.001; Figures 2B-C). In multivariate analyses with IPI, both PD-1⁺CD3⁺CD4⁺ and PD-1⁺CD3⁺CD8⁺ T-cell counts maintained an independent association with OS (Table 4). When the patients treated in the pre-rituximab era were removed from the analyses, low number of PD-1⁺ T-cells maintained their adverse impact on survival (PD1⁺CD3⁺CD4⁺ cells, ≤8.50%, the lowest tertile; OS, p=0.001 and PD1⁺CD3⁺CD8⁺ cells, ≤11.02%, the lowest tertile; OS, p=0.034; Supplementary Figure 2B-C).

Discussion

In this study, we applied mIHC and digital image analysis to a TMA comprised of PTL tissue from 74 patients. We show that PTL microenvironment contains a heterogeneous TAM population. Among these, PD-L1⁺ TAMs were the predominant subpopulation, and high infiltration of PD-L1⁺CD68⁺ TAMs associated with favorable survival. Additionally, PD-1⁺ CD4⁺ and CD8⁺ TIL contents

correlated with PD-L1⁺ TAM infiltration and survival, and both PD-L1⁺ TAMs and PD-1⁺ TILs emerged as independent indicators of survival for the patients with PTL. In contrast, neither PD-L1⁺ lymphoma cells, other PD-L1⁺ cells than TAMs nor other TAM phenotypes correlated with survival. The findings highlight the specific roles of TAMs, TILs and PD1-PD-L1 axis in regulating survival and therapy resistance in PTL.

mIHC is a novel technology enabling multi-parametric readout from a single tissue section. In our study, the simultaneous use of multiple markers is important in many ways. First, while PD-L1 was found to be expressed both in TAMs and B-cells including lymphoma cells, the prognostic impact of PD-L1 positivity was restricted to TAMs. Thus, the use of just one marker would not be able to detect the survival association. Second, the spatial relationships between TILs, TAMs and lymphoma cells are retained in our experimental strategy, allowing for a more precise appreciation of their biological interactions. Third, since mIHC was performed on all evaluable PTL tissue areas on the TMA, thereby providing an overall snapshot of the PTL microenvironment, we can avoid a bias of earlier observations focusing only on hot spot areas of immune cell counts using single marker immunohistochemistry. However, it should be noted that while the overall infiltration of PD-L1⁺ TAMs and PD-1⁺ TILs had a significant impact on survival, their functional statuses remain to be explored. Combining our panel with other multiplex panels for immunoregulatory molecules, such as FoxP3, LAG-3 or IDO-1 and IDO-2, may be useful in the evaluation of response to immunotherapy.

As described in a recent review article by Xu-Monette et al. the PD-L1 expression in the tumor microenvironment has not been previously well defined in B-cell lymphomas, and association with survival has not been demonstrated.¹⁸ PD-1 is a protein, which is classically upregulated upon

activation of T-lymphocytes. Interaction between PD-1 and PD-L1 was previously thought to induce immune tolerance by leading T-lymphocytes to apoptosis.²⁶ Further studies have, however, revealed that the expression of PD-L1 on tumor cells can lead to immune escape, to T-cell exhaustion and a state of non-responsiveness, further enabling immune escape of the tumor cells.²⁷⁻²⁹ Moreover, in addition to binding to PD-1, PD-L1 and PD-L2 can also bind to CD80/B7-1 (PD-L1)^{30, 31} and RGMb (PD-L2),³² indicating that the PD-1 – PD-L1 pathway is much more complex than previously anticipated.¹⁸

In addition to PD-L1, macrophages express PD-1.^{33, 34} Recently, Gordon and coworkers showed that PD-1 expression by TAMs inhibits phagocytosis and tumor immunity.³⁵ In addition, they demonstrated that blockade of PD-1 – PD-L1 interaction increases macrophage phagocytosis, reduces tumor growth and lengthens survival in mouse models of colon cancer, suggesting PD-1 – PD-L1 pathway having a significant role in TAM function and tumor survival.

Based on our findings, we suggest that the PD-1 - PD-L1 signaling between TAMs and TILs has clinical relevance in PTL. As PD-1 engagement on T-cells to its ligands has been linked to decreased anti-tumor immunity, and early experience on PD-1 blockade in PTL has shown promising results,³⁶ the association of high PD-L1⁺ TAM and PD-1⁺ T-cell count with favorable outcome in response to immunochemotherapy seems paradoxical. Yet, the interaction of PD-L1⁺ TAMs and PD-1⁺ T-cells might modify the tumor microenvironment in PTL, or otherwise promote an anti-tumor immune response following immunochemotherapy.

In conclusion, we argue that high PD-L1⁺ TAM and PD-1⁺ T-cell counts correlate with each other and with favorable outcome in patients with PTL. Higher PD-L1⁺CD68⁺ TAM scores seem to protect

the patients from progression and death, and identify a group of patients with favorable prognosis. Interestingly, apart from PD-L1⁺CD68⁺ TAMs, no association was found between other PD-L1⁺ cells or PD-L1⁻ TAMs and survival. Together, the data demonstrate that the PD-1 - PD-L1 axis in PTL affects the survival of patients with PTL.

References

1. Deng L, Xu-Monette ZY, Loghavi S, et al. Primary testicular diffuse large B-cell lymphoma displays distinct clinical and biological features for treatment failure in rituximab era: a report from the International PTL Consortium. *Leukemia*. 2016;30(2):361-372.
2. Twa DDW, Mottok A, Savage KJ, Steidl C. The pathobiology of primary testicular diffuse large B-cell lymphoma: Implications for novel therapies. *Blood Rev*. 2018;32(3):249-255.
3. Frick M, Bettstetter M, Bertz S, et al. Mutational frequencies of CD79B and MYD88 vary greatly between primary testicular DLBCL and gastrointestinal DLBCL. *Leuk Lymphoma*. 2018;59(5):1260-1263.
4. Chapuy B, Roemer MG, Stewart C, et al. Targetable genetic features of primary testicular and primary central nervous system lymphomas. *Blood*. 2016;127(7):869-881.
5. Menter T, Ernst M, Drachneris J, et al. Phenotype profiling of primary testicular diffuse large B-cell lymphomas. *Hematol Oncol*. 2014;32(2):72-81.
6. Twa DD, Mottok A, Chan FC, et al. Recurrent genomic rearrangements in primary testicular lymphoma. *J Pathol*. 2015;236(2):136-141.
7. Kridel R, Telio D, Villa D, et al. Diffuse large B-cell lymphoma with testicular involvement: outcome and risk of CNS relapse in the rituximab era. *Br J Haematol*. 2017;176(2):210-221.
8. Vitolo U, Chiappella A, Ferreri AJ, et al. First-line treatment for primary testicular diffuse large B-cell lymphoma with rituximab-CHOP, CNS prophylaxis, and contralateral testis irradiation: final results of an international phase II trial. *J Clin Oncol*. 2011;29(20):2766-2772.
9. Tokiya R, Yoden E, Konishi K, et al. Efficacy of prophylactic irradiation to the contralateral testis for patients with advanced-stage primary testicular lymphoma: an analysis of outcomes at a single institution. *Int J Hematol*. 2017;106(4):533-540.
10. Zucca E, Conconi A, Mughal TI, et al. Patterns of outcome and prognostic factors in primary large-cell lymphoma of the testis in a survey by the International Extranodal Lymphoma Study Group. *J Clin Oncol*. 2003;21(1):20-27.
11. Cheah CY, Wirth A, Seymour JF. Primary testicular lymphoma. *Blood*. 2014;123(4):486-493.
12. Lenz G, Wright G, Dave SS, et al. Stromal gene signatures in large-B-cell lymphomas. *N Engl J Med*. 2008;359(22):2313-2323.
13. Riihijarvi S, Fiskvik I, Taskinen M, et al. Prognostic influence of macrophages in patients with diffuse large B-cell lymphoma: a correlative study from a Nordic phase II trial. *Haematologica*. 2015;100(2):238-245.

14. Kiyasu J, Miyoshi H, Hirata A, et al. Expression of programmed cell death ligand 1 is associated with poor overall survival in patients with diffuse large B-cell lymphoma. *Blood*. 2015;126(19):2193-2201.
15. Kwon D, Kim S, Kim PJ, et al. Clinicopathological analysis of programmed cell death 1 and programmed cell death ligand 1 expression in the tumour microenvironments of diffuse large B cell lymphomas. *Histopathology*. 2016;68(7):1079-1089.
16. Goodman A, Patel SP, Kurzrock R. PD-1-PD-L1 immune-checkpoint blockade in B-cell lymphomas. *Nature reviews Clinical oncology*. 2017;14(4):203-220.
17. Eyre TA, Collins GP. Immune checkpoint inhibition in lymphoid disease. *Br J Haematol*. 2015;170(3):291-304.
18. Xu-Monette ZY, Zhou J, Young KH. PD-1 expression and clinical PD-1 blockade in B-cell lymphomas. *Blood*. 2018;131(1):68-83.
19. Carey CD, Gusenleitner D, Lipschitz M, et al. Topological analysis reveals a PD-L1 associated microenvironmental niche for Reed-Sternberg cells in Hodgkin lymphoma. *Blood*. 2017;130(22):2420-2430.
20. Powles T, Eder JP, Fine GD, et al. MPDL3280A (anti-PD-L1) treatment leads to clinical activity in metastatic bladder cancer. *Nature*. 2014;515(7528):558-562.
21. Lau J, Cheung J, Navarro A, et al. Tumour and host cell PD-L1 is required to mediate suppression of anti-tumour immunity in mice. *Nat Commun*. 2017;8:14572.
22. Blom S, Paavolainen L, Bychkov D, et al. Systems pathology by multiplexed immunohistochemistry and whole-slide digital image analysis. *Sci Rep*. 2017;7(1):15580.
23. Swerdlow SH, Campo E, Harris NL, et al. WHO Classification of Tumours of Haematopoietic and Lymphoid Tissues, Revised Fourth Edition. 2017; Volume 2.
24. Carpenter AE, Jones TR, Lamprecht MR, et al. CellProfiler: image analysis software for identifying and quantifying cell phenotypes. *Genome Biol*. 2006;7(10):R100.
25. Leivonen S-K, Pollari M, Brück O, et al. Clinical impact of the T/NK-Cell Signature Predicts Poor Survival in Patients with Primary Testicular and Diffuse Large B-Cell Lymphomas. *Blood*. 2017;130 (Suppl 1):#4027.
26. Dong H, Strome SE, Salomao DR, et al. Tumor-associated B7-H1 promotes T-cell apoptosis: a potential mechanism of immune evasion. *Nat Med*. 2002;8(8):793-800.
27. Wherry EJ, Kurachi M. Molecular and cellular insights into T cell exhaustion. *Nat Rev Immunol*. 2015;15(8):486-499.

28. Pardoll DM. The blockade of immune checkpoints in cancer immunotherapy. *Nat Rev Cancer*. 2012;12(4):252-264.
29. Pauken KE, Wherry EJ. Overcoming T cell exhaustion in infection and cancer. *Trends Immunol*. 2015;36(4):265-276.
30. Butte MJ, Keir ME, Phamduy TB, Sharpe AH, Freeman GJ. Programmed death-1 ligand 1 interacts specifically with the B7-1 costimulatory molecule to inhibit T cell responses. *Immunity*. 2007;27(1):111-122.
31. Park JJ, Omiya R, Matsumura Y, et al. B7-H1/CD80 interaction is required for the induction and maintenance of peripheral T-cell tolerance. *Blood*. 2010;116(8):1291-1298.
32. Xiao Y, Yu S, Zhu B, et al. RGMB is a novel binding partner for PD-L2 and its engagement with PD-L2 promotes respiratory tolerance. *J Exp Med*. 2014;211(5):943-959.
33. Huang X, Venet F, Wang YL, et al. PD-1 expression by macrophages plays a pathologic role in altering microbial clearance and the innate inflammatory response to sepsis. *Proc Natl Acad Sci U S A*. 2009;106(15):6303-6308.
34. Bally AP, Lu P, Tang Y, et al. NF-kappaB regulates PD-1 expression in macrophages. *J Immunol*. 2015;194(9):4545-4554.
35. Gordon SR, Maute RL, Dulken BW, et al. PD-1 expression by tumour-associated macrophages inhibits phagocytosis and tumour immunity. *Nature*. 2017;545(7655):495-499.
36. Nayak L, Iwamoto FM, LaCasce A, et al. PD-1 blockade with nivolumab in relapsed/refractory primary central nervous system and testicular lymphoma. *Blood*. 2017;129(23):3071-3073.

Table 1. Patient and treatment characteristics.

	All n (%)	PDL1+ CD68+ low	PD-L1+ CD68+ intermed.	PD-L1+ CD68+ high	<i>p</i>
Number of patients	74	25 (34)	24 (32)	25 (34)	
Median age (range)	70 (36-92)	68 (38-86)	73 (37-92)	66 (46-90)	
Age					
≤60, years	17 (23)	6 (24)	4 (17)	7 (28)	0.638
>60, years	57 (77)	19 (76)	20 (83)	18 (72)	
Molecular subgroup					
GCBa	17 (23)	8 (32)	4 (17)	5 (20)	0.426
Non-GCB	56 (76)	17 (68)	20 (83)	19 (76)	
NA	1 (1)			1 (4)	
Stage					
I-II	47 (64)	10 (40)	16 (67)	21 (84)	0.002
III-IV	24 (32)	15 (60)	6 (25)	3 (12)	
NA	3 (4)		2 (8)	1 (4)	
IPI score					
0-2	50 (68)	13 (52)	17 (71)	20 (80)	0.065
3-5	20 (27)	11 (44)	5 (21)	4 (16)	
NA	4 (5)	1 (4)	2 (8)	1 (4)	
CNS prophylaxis	36 (49)	9 (36)	11 (46)	16 (64)	0.137
IV prophylaxis	34 (46)	8 (32)	10 (42)	16 (64)	0.057
IT prophylaxis	7 (9)	2 (8)	3 (13)	2 (8)	0.856
Contralateral testis treated	23 (31)	6 (24)	7 (29)	10 (40)	0.464
Irradiation	12 (16)	2 (8)	3 (13)	7 (28)	0.136
Surgical excision	11 (15)	4 (16)	4 (17)	3 (12)	0.884
Anthracycline-based chemotherapy	60 (81)	18 (72)	21 (88)	21 (84)	0.305
Treated with rituximab	35 (47)	9 (36)	11 (46)	15 (60)	0.237
Relapse of contralateral testis	1 (1)	0 (0)	1 (4)	0 (0)	0.377
CNS progression	9 (12)	4 (16)	4 (17)	1 (4)	0.312

^aGCB, germinal center B-cell like; NA, not applicable; IPI, International prognostic Index; CNS, central nervous system; IV, intravenous; IT, intrathecal; p, p-value determined by Kruskal-Wallis test.

Table 2. Cox regression analysis at the univariate level showing association of gene expression levels with overall survival.

Gene symbol	HR ^a	95% CI	<i>p</i>
<i>CD68</i>	0.505	0.290-0.881	0.016
<i>CD274</i>	0.737	0.592-0.919	0.007
<i>PDCD1LG2</i>	0.688	0.505-0.936	0.017
<i>PDCD1</i>	0.846	0.659-1.088	0.192
<i>CD163</i>	0.914	0.636-1.313	0.627
<i>MAF</i>	0.899	0.551-1.466	0.668

^aHR, hazard ratio; CI, confidence interval. Boldface font indicates statistical significance ($p < 0.05$).

Table 3. Cox regression analysis at the univariate level showing association of cell immunophenotypes with overall survival.

Cell immunophenotype	HR ^a	95% CI	<i>p</i>
PD-L1 ⁺	0.983	0.967-0.999	0.038
CD20 ⁺	1.009	0.995-1.023	0.209
PD-L1 ⁺ CD20 ⁺	0.993	0.978-1.008	0.376
PD-L1 ⁺ CD68 ⁻	0.981	0.955-1.007	0.146
CD68 ⁺	0.986	0.964-1.008	0.196
PD-L1 ⁺ CD68 ⁺	0.965	0.933-0.999	0.042
PD-L1 ⁺ CD68 ⁺ /CD68 ⁺	0.987	0.975-0.998	0.027
PD-L1 ⁻ CD68 ⁺	1.012	0.982-1.043	0.437
CD68 ⁺ c-Maf ⁺	0.835	0.668-1.044	0.113
PD-L1 ⁺ CD68 ⁺ c-Maf ⁺	0.734	0.518-1.041	0.083
CD163 ⁺	0.996	0.978-1.014	0.666
PD-L1 ⁺ CD163 ⁺	0.989	0.969-1.010	0.298
CD3 ⁺	0.194	0.053-0.712	0.013
PD-1 ⁺ CD3 ⁺ CD4 ⁺	0.089	0.008-0.999	0.050
PD-1 ⁺ CD3 ⁺ CD8 ⁺	0.042	0.003-0.537	0.015

^aHR, hazard ratio; CI, confidence interval; PD-L1⁺CD68⁺ implies the number of PD-L1⁺CD68⁺ TAMs from all cells; PD-L1⁺CD68⁺/CD68⁺ implies the number of PD-L1⁺CD68⁺ TAMs from all CD68⁺ TAMs. Boldface font indicates statistical significance (p<0.05).

Table 4. Cox regression analysis at the multivariate level showing independent association of low cell immunophenotypes and IPI high (IPI 3-5) with overall survival.

Cell immunophenotype	HR ^a	95% CI	<i>p</i>
PD-L1 ⁺ CD68 ⁺	2.214	1.054-4.650	0.036
IPI	4.325	2.008-9.312	<0.001
PD-L1 ⁺ CD68 ⁺ /CD68 ⁺	2.275	1.054-4.909	0.036
IPI	3.608	1.643-7.923	0.001
PD-1 ⁺ CD3 ⁺ CD4 ⁺	2.654	1.261-5.586	0.010
IPI	4.907	2.275-10.585	<0.001
PD-1 ⁺ CD3 ⁺ CD8 ⁺	2.259	1.075-4.748	0.031
IPI	4.971	2.314-10.678	<0.001

^aHR, hazard ratio; CI, confidence interval; IPI, International Prognostic Index

Figure legends

Figure 1. Characterization of cell immunophenotypes with mIHC. A-C) Representative images from 4-plex mIHC stainings. Panels (low, intermediate, and high) show representative images from the corresponding tertiles, based on the content of different immune cell subtypes. The insets highlight cells with higher magnification. PD-L1=blue, PD-L2=red, CD68=white, c-Maf=green (A); PD-L1=blue, CD163=red, CD20=white, PD1=green (B); CD3=blue, CD8=red, CD4=white, PD1=green (C). Scale bar 40 μ m. D) Proportions of distinct immune cell subpopulations from all cells. PD-L1⁺CD68⁺ indicating the content of PD-L1⁺ TAMs, PD-L1⁺CD163⁺ and PD-L1⁺CD68⁺c-Maf⁺ the content of PD-L1⁺ M2-polarized TAMs, PD-1⁺CD3⁺CD4⁺ and PD-1⁺CD3⁺CD8⁺ the content of PD-1⁺ TILs, and PD-L1⁺CD20⁺ the content of PD-L1⁺ lymphoma cells.

Figure 2. Association of the immune cell subtypes with survival. A-C) Cell immunophenotypes were determined by mIHC from 74 PTL patients. Patients were stratified into three equal subgroups (high, intermediate and low) based on tertiles of PD-L1⁺CD68⁺ TAM, PD-1⁺CD3⁺CD4⁺ T-cell, and PD-1⁺CD3⁺CD8⁺ T-cell counts. Kaplan-Meier plots depict survival differences between the PD-L1⁺CD68⁺ (A), PD-1⁺CD3⁺CD4⁺ (B), and PD-1⁺CD3⁺CD8⁺ (C) groups. P-values were determined by univariate Cox regression analysis (HR, hazard ratio with 95% confidence interval).

Figure 1

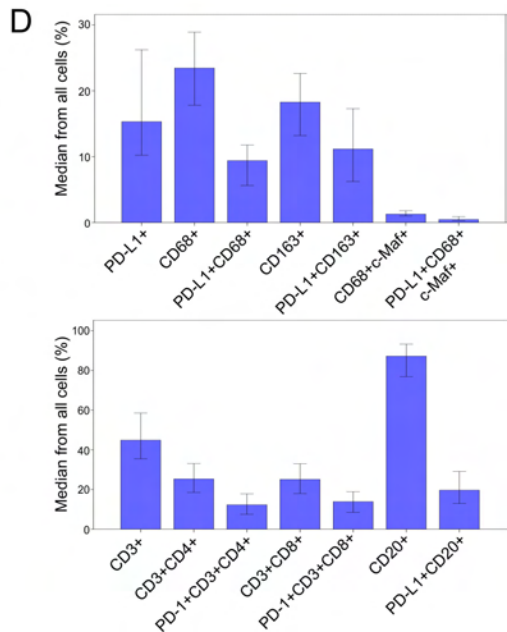
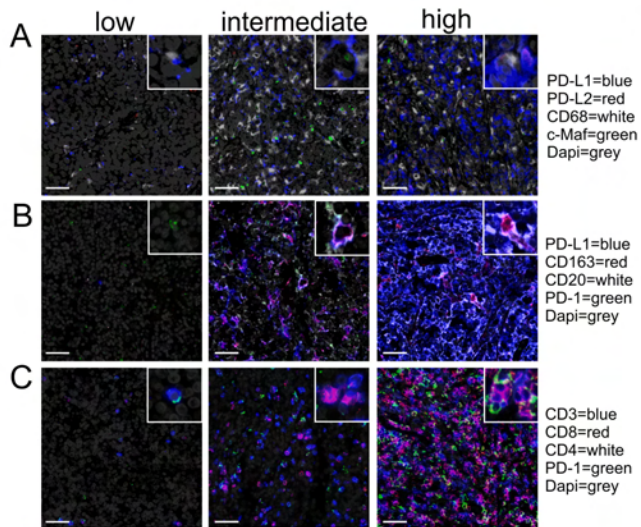
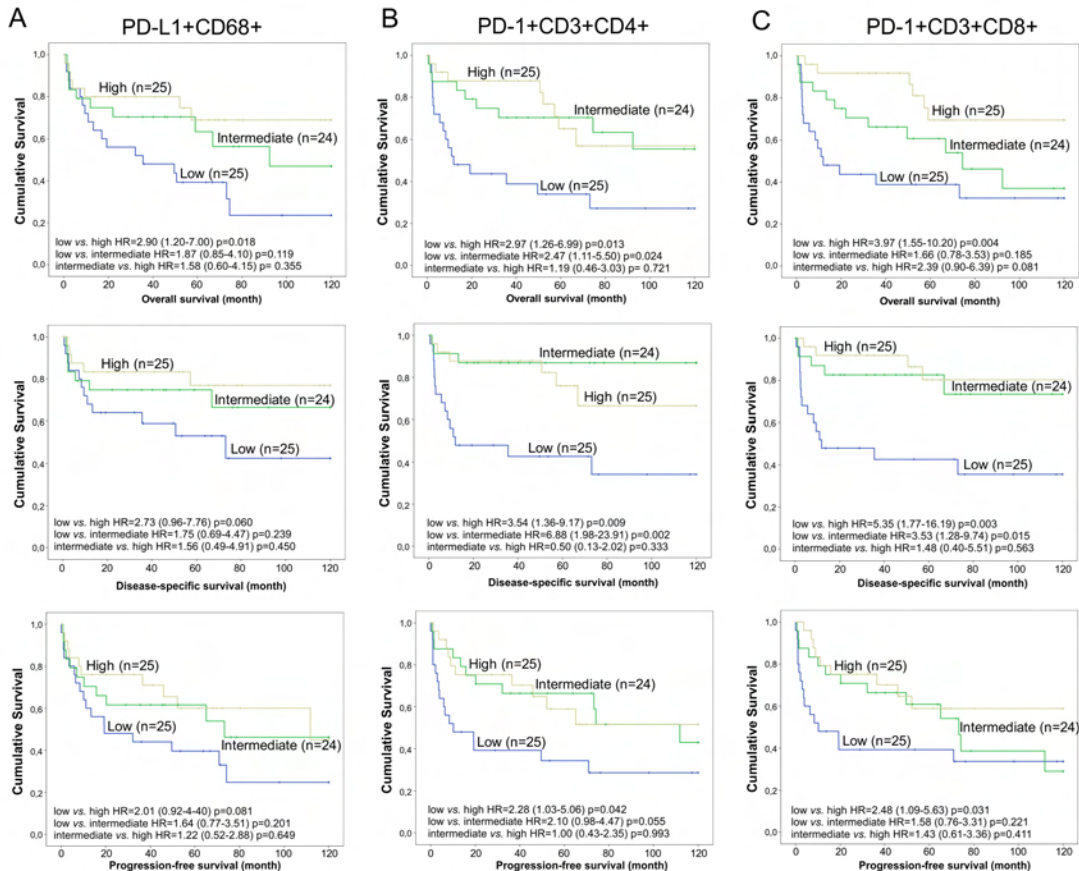


Figure 2



Supplementary material

PD-L1⁺ tumor-associated macrophages and PD-1⁺ tumor infiltrating lymphocytes predict survival in primary testicular lymphoma

Marjukka Pollari^{1,2}, Oscar Brück³, Teijo Pellinen⁴, Pauli Vähämurto^{1,5}, Marja-Liisa Karjalainen-Lindsberg⁶, Susanna Mannisto^{1,5}, Olli Kallioniemi^{4,7}, Pirkko-Liisa Kellokumpu-Lehtinen^{2,8}, Satu Mustjoki^{3,9}, Suvi-Katri Leivonen^{1,5} and Sirpa Leppä^{1,5}

¹*Research Program Unit, Faculty of Medicine, University of Helsinki, Helsinki, Finland;*

²*Department of Oncology, Tampere University Hospital, Tampere, Finland;*

³*Hematology Research Unit Helsinki, Department of Clinical Chemistry and Hematology, University of Helsinki, Helsinki, Finland;*

⁴*Institute for Molecular Medicine Finland (FIMM), Helsinki, Finland;*

⁵*Department of Oncology, Comprehensive Cancer Center, Helsinki University Hospital, Helsinki, Finland;*

⁶*Department of Pathology, Helsinki University Hospital, Helsinki, Finland;*

⁷*Science for Life Laboratory, Karolinska Institutet, Department of Oncology and Pathology, Solna, Sweden;*

⁸*Faculty of Medicine and Life Sciences, University of Tampere, Tampere, Finland;*

⁹*Department of Hematology, Comprehensive Cancer Center, Helsinki University Hospital, Helsinki, Finland*

Supplementary methods

Multiplex Immunohistochemistry (mIHC)

General. TMA blocks were cut in 3.5 µm sections on objective slides, which were dried overnight at +37°C and stored for short-term use at +4°C. All consecutive phases were performed in room temperature unless otherwise specified. Protein blocking and antibody incubations were performed in a humid chamber. Slides were washed three times with 0.1% Tween-20 (Thermo Fisher Scientific) diluted in 10 mM Tris-HCL buffered saline pH 7.4 (TBS) after peroxide block, antibody incubations, and fluorochrome reaction. The primary antibodies are listed in Supplementary Table 1.

Tissue preparation. Slides were deparaffinized in xylene and rehydrated in graded ethanol series and H₂O. Heat-induced epitope retrieval (HIER) was carried out in 10 mM Tris-HCl - 1 mM EDTA buffer (pH 9) in +99°C for 20 min (PT Module, Thermo Fisher Scientific, Waltham, MA). Peroxide activity was blocked in 0.9% H₂O₂ solution for 15 min, and protein block performed with 10% normal goat serum (TBS-NGS) for 15 min.

Fluorescence staining. Primary antibodies were diluted in protein blocking solution and incubated for 1 h 45 min. Thereafter, secondary anti-mouse or anti-rabbit horseradish peroxidase-conjugated (HRP) antibodies (Immunologic, Netherlands) diluted 1:1 with washing buffer were applied for 45 min. Tyramide signal amplification (TSA) Alexa Fluor 488 (PerkinElmer, Waltham, MA) diluted in TBS was applied on the slides for 10 min. Primary antibodies were denatured and enzymatic activity of secondary antibody HRP was quenched by repeating HIER. Thereafter, peroxide and protein block were repeated, followed by application of a different primary antibody, matching HRP-conjugated secondary antibody diluted 1:3 with washing buffer and TSA Alexa Fluor 555 (PerkinElmer). Again, HIER, peroxide block and protein block were repeated. Then, the slides were incubated with two additional primary antibodies immunized in different species overnight in +4°C. Next, AlexaFluor647 and AlexaFluor750 fluorochrome-conjugated secondary antibodies (Thermo Fisher Scientific) diluted in 1:150 and DAPI (Roche) counterstain diluted 1:250 in washing buffer were applied for 45 min. Last, we applied ProLong Gold mountant (Thermo Fisher Scientific) and a coverslip on the slides.

Denaturation test. In order to minimize false positive signal from antibody cross-reactions during the mIHC procedure, we required that primary antibodies selected for mIHC must be completely denatured during the HIER step between staining rounds. Therefore, the denaturation properties of all primary antibodies were examined by performing an additional HIER step between primary and secondary antibody incubation. Antibodies not denaturing completely were detected with Cy5 and Cy7 fluorescence probes, which do not require denaturation.

Imaging. Fluorescent images were acquired with the AxioImager.Z2 (Zeiss, Germany) microscope equipped with Zeiss Plan-Apochromat 20x objective (NA 0.8), CoolCube1 CCD camera (MetaSystems, Germany), PhotoFluor LM-75 (89 North) metal-halide light source and Zeiss EPLAX VP232-2 power supply. DAPI, FITC, Cy3, Cy5, and Cy7 filters with compatible LED light sources were used and exposure times for all fluorescence channels were optimized visually for fluorescence imaging. Scanned images were acquired and were converted to JPEG2000 format (95% quality) for image analysis to reduce memory demand.

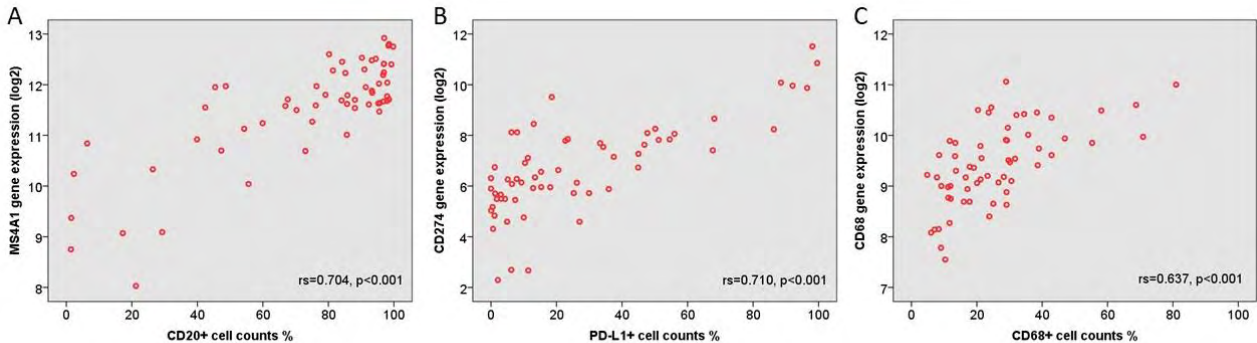
Image analysis. The quality of gray-scale images of each TMA spot was first assessed and few images were discarded due to blurred focusing or unsuccessful image registration caused mainly by air bubbles in mounting media or shattered tissue, respectively. In the image analysis, DAPI-

counterstained nuclei were segmented with adaptive Otsu thresholding, clumped objects separated by intensity patterns and cells segmented with nuclei contour expansion. We used the machine-learning platform CellProfiler 2.1.2 for cell segmentation, intensity measurements (upper quartile intensity) and immune cell classification. We computed marker colocalization with the single-cell analysis software FlowJo v10 (FlowJo LLC.). The optimal gate coordinates were ensured by visualising matching cells with CellProfiler.

Data analysis Spots with less than 5000 cells were excluded from the analysis. Different cell types were quantified as proportion to all cells (e.g. number of CD68⁺PD-L1⁺ TAMs to all cells in a TMA spot). Duplicate spots from the same patient were merged by the mean value of each cell type and their immunophenotype.

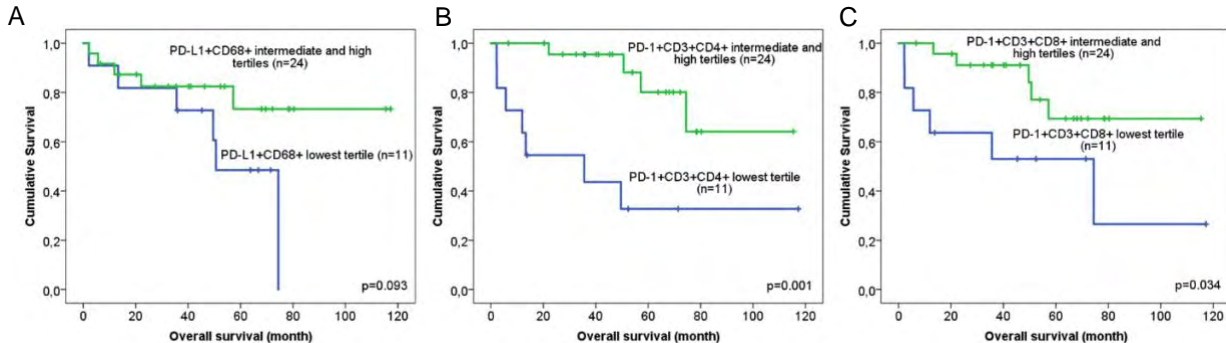
Supplementary Figures

Supplementary Figure 1.



Correlation between gene expression and immunohistochemistry (IHC). A-C) Correlations between *MS4A1* (A), *CD274* (B), and *CD68* (C) mRNA levels with the corresponding cell counts in mIHC were determined by Spearman rank analysis.

Supplementary Figure 2.



Association of the immune cell subtypes with survival among the rituximab treated patients. Cell immunophenotypes were determined by mIHC from 35 PTL patients treated with rituximab. Patients were stratified into three equal subgroups (high, intermediate and low), based on tertiles of PD-L1+CD68+ TAM, PD-1+CD3+CD4+ T-cell, and PD-1+CD3+CD8+ T-cell counts, and the intermediate and high groups were merged based on the data from the whole cohort of 74 patients. Kaplan-Meier plots depict survival differences between the PD-L1+CD68+ (A), PD-1+CD3+CD4+ (B), and PD-1+CD3+CD8+ (C) groups.

Supplementary tables

Supplementary Table 1. Antibody panels.

Theme	GFP	Cy3	Cy5	Cy7
T-cells	PD1 ^a	CD3	CD8	CD4
Macrophages	c-MAF	PD-L1	PD-L2	CD68
B-cells and macrophages	PD-1	PD-L1	CD163	CD20

^aAntibodies: PD-1 (clone PDCD1) LsBio, CD3 (clone EP449E) Abcam, CD8 (clone C8/144B) Abcam, CD4 (clone EPR6855) Abcam, cMAF (clone EPR16484) Abcam, PD-L1 (clone E1L3N) Cell Signaling, PD-L2 (polyclonal) Sigma, CD68 (clone KP1) Abcam, CD20 (clone L26) BioSB, CD163 (clone EPR14643), Abcam.

Supplementary Table 2. Correlations of the PD-1⁺ TIL and PD-L1⁺ TAM counts.

Cell immunophenotype	Spearman rho	p-val
CD3 ⁺ CD4 ⁺ vs. PD-L1 ⁺ CD68 ⁺	0.699	<0.001
CD3 ⁺ CD8 ⁺ vs. PD-L1 ⁺ CD68 ⁺	0.640	<0.001
PD-1 ⁺ CD3 ⁺ CD4 ⁺ vs. PD-L1 ⁺ CD68 ⁺	0.496	<0.001
PD-1 ⁺ CD3 ⁺ CD8 ⁺ vs. PD-L1 ⁺ CD68 ⁺	0.461	<0.001